Physical Chemistry: An Indian Journal

Research | Vol17 Iss3

Studies the Effect of Pressure on Electrical Conductivity of Non-Stochiometry Cuprous Bromide in Solid State

Vimalesh Kumar Singh*

Department of Chemistry, Faculty of Science, Dr. Ambedkar Govt. P.G. College Unchahar Rae Bareli Uttar Pradesh India

***Corresponding author**:Vimalesh Kumar Singh, Department of Chemistry, Faculty of Science Dr. Ambedkar Govt. P.G. College, India; Email: drvksinghlu@rediffmail.com

Received date: June 26, 2022, Manuscript No. TSPC-22-67752; **Editor assigned:** June 29, 2022, PreQC No. TSPC-22-67752 (PC); **Reviewed:** July 13, 2022, QC No. TSPC -22-67752(Q); **Revised:** August 25, 2022, Manuscript No. TSPC-22-67752 (R); **Published:** September 05, 2022, DOI: 10.37532/ 0974-7524.2022. 17(3).167

Abstract

The electrical conductivity (d.c.) of the solid CuBr with a definite stoichiometry was determined employing cell configuration Cu / CuBr / Cu over an extensive range of pressure which allowed us to obtain the detail runs of conductivity, including the phase transformations: γ-CuBr ↔β-CuBr and β--CuBr ⇔ α-CuBr. Conductivity decreases with increases in the concentration of bromide in CuBr lattice. Conductivity of CuBr, CuBr1.0018, and CuBr1.0037 are increases with increasing thickness as well as pressure. The increase of conductivity (σ) with thickness is surprising. With available information, we suggest that the lower conductivity of the stacked pellet of the same thickness is due to larger contact resistance in stacked pellet.

Keywords: ***Conductivity; Definite stoichiometry; Stacked pellet; Graphite coated pellet; Phase transformation***

Introduction

The conductivity measurement of CuBr has been an important topic of research for decades [1-6]. The electrical conductivity of cuprous bromide was first studied by Friederich and Meyer, who suggested that CuBr shows metallic-type conduction [7]. Rapoport and Pistorius reported as the phase diagrams of CuBr to 40 kbar consist of three solid phases and the liquid [8]. The stability region of hexagonal CuBr is terminated at 6.1 kbar. At higher pressures, there is a direct transition from the zinc-blende structure to disordered bcc. The melting curves of the disordered bcc phases of CuBr at first rise steeply with pressure, but flatten off considerably above ~ 25 and ~ 30 kbar, respectively. This is ascribed to the presence of a denser species in the melt. Van-Valkenburg found two transitions, separated by ~ 0.1 kbar, at 47 kbar. The phase with the narrow stability range was non-cubic, while the higher pressure form was cubic [9] . In addition, there was a transition at 80 kbar to a non-cubic form [10]. Edwards and Drickamer found two transitions at ~ 50 kbar, separated by ~ 2.5 kbar, and two further transitions at 80 kbar and 95 kbar. The sensitivity of conductivity with contact pressure in our sample aroused our curiosity to measure conductivity with a definite pressure. Measurement of conductivity of CuBr of definite stoichiometry with pressure does not seem to be available in literature though there are several reports on phase transition in CuBr. Jayaramann et al, reported that the phase transition of CuBr employing volumetric, conductivity, polarization, and optical techniques [11]. In their studies, CuBr has been found to have three stable phases below 20 kbar. On the basis of optical and X-rays diffraction studies, Moore et al, reported that the phase transition at 4 kbar and 5 kbar [12]. They also reported a sluggish phase at 14 kbar-30 kbar and other at 53 kbar. These transitions were later verified by resistivity measurements [13, 14]. A relevant review of the literature reveals that significant work has been done on the structural and transport properties of solid and molten CuBr in order to analyze the structure and ionic motion in different phases [15-21]. However, some detailed experimental data are still desirable. Cuprous halides are interesting from both scientific and technological points of view. Moreover, economically, copper compounds might be a good alternative to silver conductors. Since, the use of CuBr for the fast ions electrolyte, due to highly mobile cuprous ions is getting popularity and this material also seems to possess

Citation: Singh V. Studies The Effect Of Pressure On Electrical Conductivity Of Non-Stochiometry Cuprous Bromide In Solid State. Phys. Chem.: Indian Jounal.2022;17(3):262.

Super Ionic Conductivity (SIC), it has its importance both academically as well as technically. Hence, the conductivity of CuBr in a low, as well as high-pressure region, including the phase transition -phase ⇔ β-phase, β-phase ⇔ α-phase, was studied in the present work.

Experimental method

Sample preparation

Cuprous bromide was prepared by treating solutions of copper sulphate-AR (Sigma) with sodium bisulphite-AR (Sigma) and potassium bromide-AR (Sigma) with continuous stirring. This solution was poured into a large beaker containing double distilled water. Cuprous bromide was precipitated and settled down. The solution of supernatant liquid in the beaker was decanted. The solid mass remaining in the beaker was rinsed with water and acetone at least 3 times to 4 times to remove as much cupric bromide and other impurities from the solution till the supernatant liquid was almost colorless. Cuprous bromide was vacuum filtered with the help of a Buckner funnel and washed with acetone and absolute alcohol while filtering. Cuprous bromide after the filtration was dried at 50°C in a vacuum oven for 10 hours and was stored in a vacuum desiccator for use. Before conductivity measurements, the product obtained was probed by Scanning Electron Microscopy (SEM), X-Ray Diffraction (XRD), and Electron Paramagnetic Resonance spectroscopy (EPR) methods.

Procedure for measuring conductivity as a function of pressure and thickness

Spherical bright copper electrodes (diameter-1.72 cm, thickness 1 mm, and area 2.32 cm^2) washed with AR acetone and dried at 40°C were employed. A2 mm thick pellet was sandwiched between two copper electrodes in order to give the cell configuration $Cu/CuBr_x/Cu$. This cell was loaded in a pressure machine (MTS model No. 810.12) through which variable pressure can be applied. The electrodes were connected with a digital conductivity meter HP 3457A model. The schematic diagram of the conductivity measuring assembly is shown in **FIG. 1**. Before applying additional pressure, measurements were made when the electrodes were just touching the pellet. This value was considered as conductivity at contact pressure. The value of external pressure was gradually increased and a corresponding change in conductivity was recorded. For thick pellets (4 mm and 6 mm) the same procedure was adopted for measuring conductivity. In some runs, pellets were damaged but such data were excluded and only those samples which did not break were taken into account for reporting conductivity data. The same procedure was adopted for measuring the contact resistance between the electrode and pellet of CuBr.

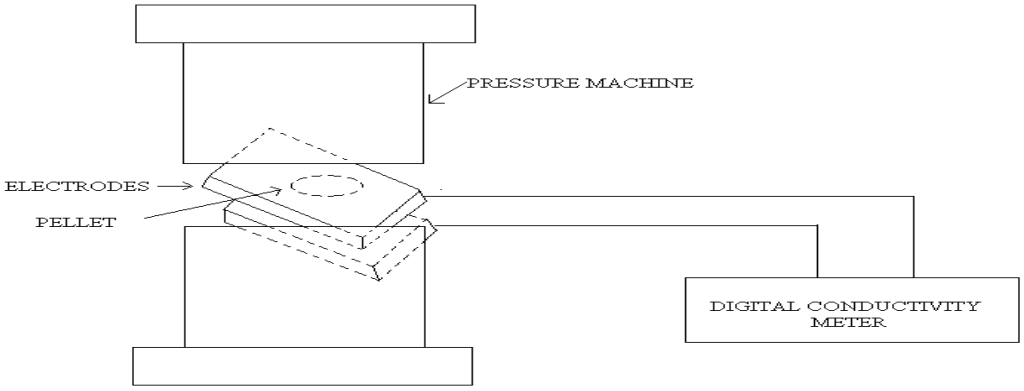

FIG. 1**. Circuit diagram for conductivity and current measurement.**

Result and Discussions

Characterization

The CuBr used in this investigation has been characterized based on the impurity present in it. Only Cu^{++} impurity has been taken into account since Cu^{++} is only an inorganic cation which is likely to play an active role in the transport properties of CuBr. Transport property is the intrinsic property of CuBr material and effective only when an impurity atom (bromine atom) enters into the lattice (of a given crystalline material) or produces any perturbation to the lattice by making an electron deficient bond in the crystal lattice. A scanning electron microscopy (SEM) image of the cross-sectional cell structure is shown in **FIG. 2.**

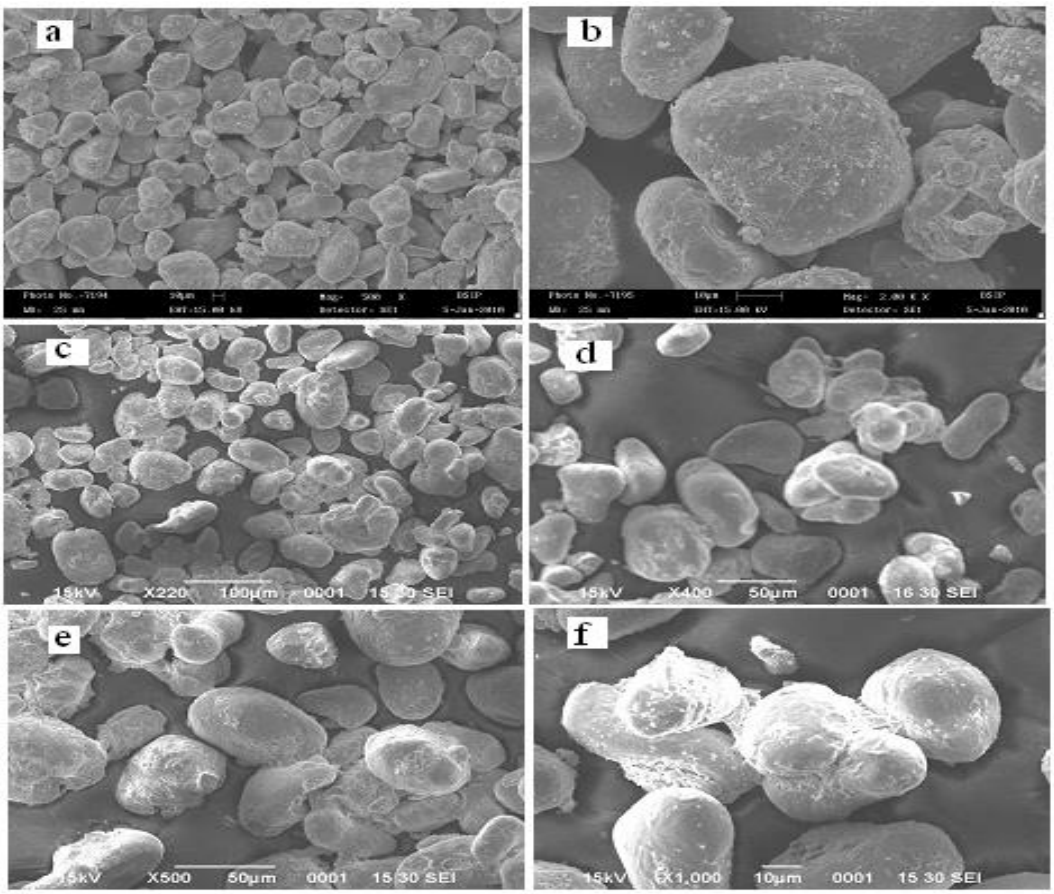

FIG. 2**. SEM images of CuBr crystals: (a and b) synthesized CuBr, (c-f) standard CuBr.**

A room temperature, X-ray powder diffraction pattern is shown in **FIG. 3** and **FIG. 4** resemble well to that of the γ −CuBr. The XRD patterns observed are in good agreement with the literature value of CuBr and the observed peaks can be attributed to the cuprous bromide γ phase. The Bragg diffraction patterns of the CuBr and $CuBr_{1.0018}$ samples showed (**FIG. 3**, **FIG. 4**) the cubic zincblende structure with lattice plane oriented along (111), (220), and (311). For CuBr, the most intense peak corresponds to the centered at 27.12°, while two other relatively less intense peaks correspond to the centered at 45.03° and 53.36° whereas in $CuBr_{1.0018,}$ the most intense peak corresponds to the centered at 27.00°, while two other relatively less intense peaks correspond to the centered at 44.90° and 53.24°. From the literature it is observed that the X-ray diffraction pattern was found to be in good agreement with the γ −CuBr patterns, indicating that the cuprous bromide is present as the γ −phase at room temperature. A comparison between the experimental and the literature-reported X-ray diffraction peak position and intensities shown are in **TABLE 1**.

TABLE 1. **A comparison of experimental and reported X-ray diffraction peak positions and intensities for CuBr.**

Phase	Literature data for CuBr (Suyal et al 2003)		Experimental data		
	2Ɵ	Intensity	Sample	2Ɵ	Intensity
111	27.12	100	CuBr	27.117	100
				45.025	34.01
220	45.02	50		53.356	17.45
			$CuBr_{1.0018}$	27.001	99.5
311	53.34	35		44.9	44.5
				53.24	34.5

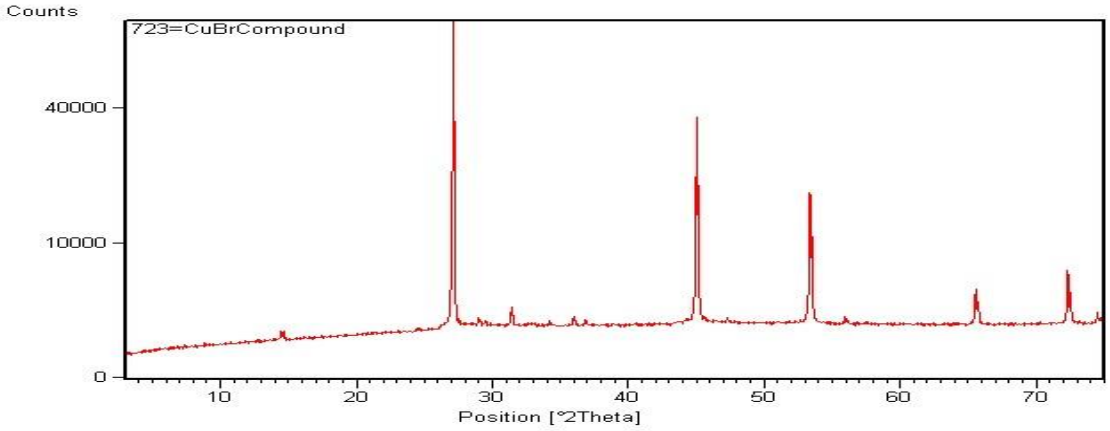

FIG. 3. **Plot illustrating the XRD pattern of γ-CuBr.**

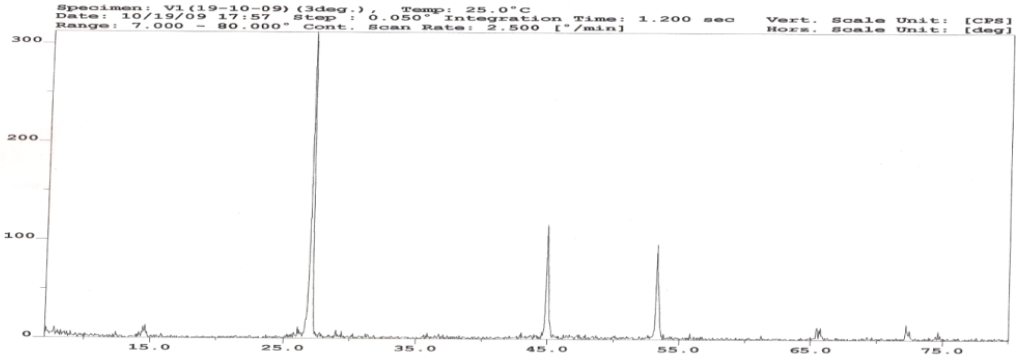

FIG. 4. **Plot illustrating the XRD pattern of γ-CuBr$_{1.0018}$.**

EPR signals were not observed in CuBr as evidenced from the EPR spectra **FIG. 5** indicate the presence of Cu^{+} in the sample. In stoichiometric cuprous bromide crystal, Cu^{+} ion and Br^{-} ion have the configuration $3d^{10}\ 4s^{0}$ and $4s^{2}\ 4p^{6}$, respectively. In the present sample of $CuBr_x$ excess bromine atoms are incorporated into a cuprous bromide lattice. Consequently, bromine atoms would interact with the electron of Cu^{+} ion, as if Cu is converted to Cu^{++} having $3d^{9}\ 4s^{0}$ configurations. This configuration creates an electron deficiency in copper of $CuBr_x$. This deficiency in copper acts as a positive hole in $CuBr_x$ crystal which is likely to play an active role in the transport properties of CuBr.

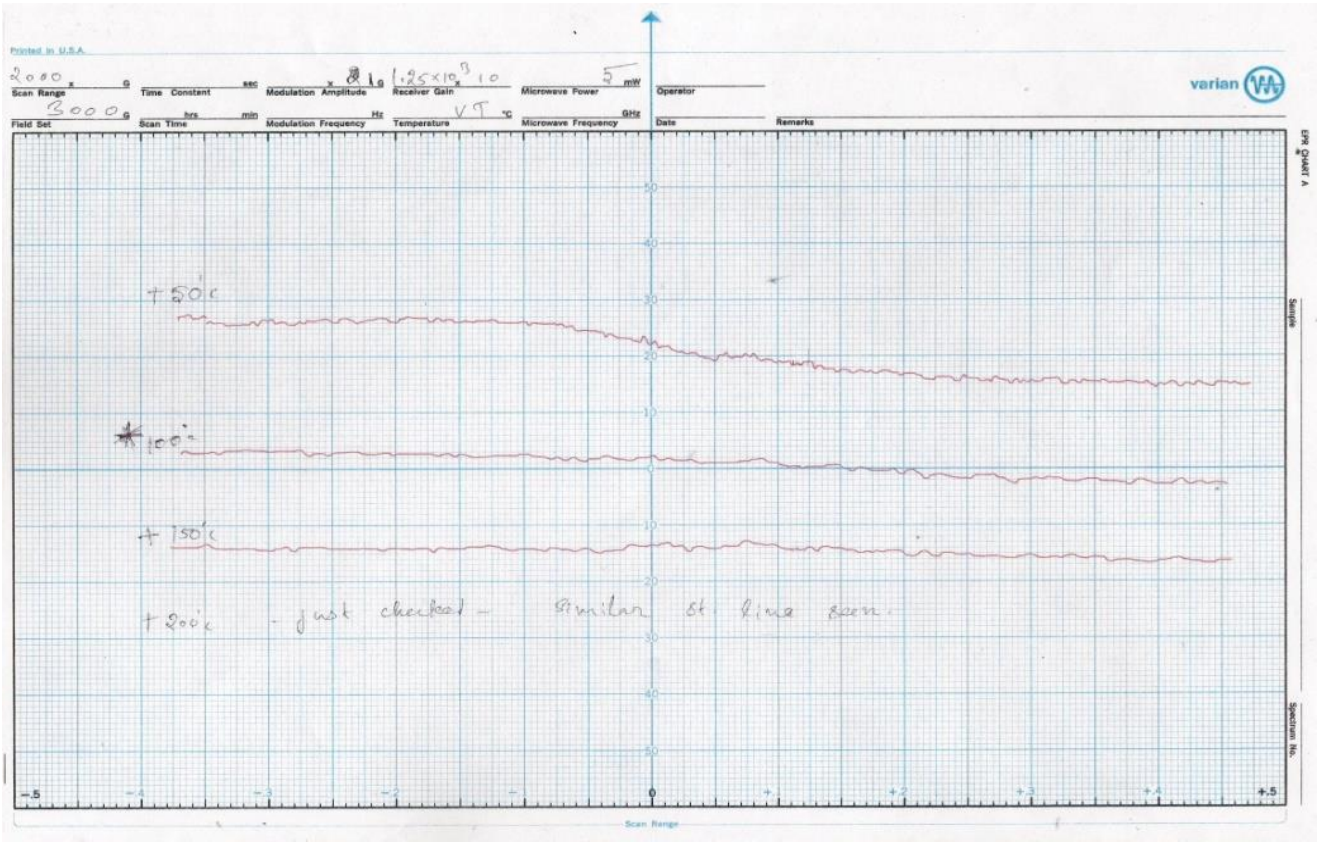

FIG. 5. **EPR spectra illustrating the presence of Cu ion in CuBr sample.**

Stoichiometric study of CuBr

Cuprous bromide used in the present investigation was analyzed by atomic adsorption spectrophotometrically for copper and bromide was determined iodometrically. The percentage of copper (**TABLE 2)** in CuBr was found to be 44.254 and 44.206, respectively, in two batches. The percentage of bromine in CuBr was found to be 57.746 and 55.795 in two **TABLE 2** batches, respectively. Thus stoichiometry of $CuBr_x$ in sample No. 1 was found to be $CuBr_{1.0018}$ whereas in sample No. 2 it was $CuBr_{1.0037.}$

TABLE 2**. Analytical Data for the Stoichiometric Determination of $CuBr_x$ (sample No. 1 & No. 2).**

Experimental d+V9:AB10ata	Amount of Copper (g/cc)		% Copper		% Bromine	
	Sample No.1	Sample No.2	Sample No.1	Sample No.2	Sample No.1	Sample No.2
1	0.44253	0.44205	44.253	44.205	55.747	55.795
2	0.88508	0.88412	44.254	44.206	55.746	55.794
3	1.32759	1.32612	44.253	44.204	55.747	55.796
4	1.77016	1.76824	44.254	44.206	55.746	55.794

The conductivity of CuBr, $(CuBr)_{1.0018}$, and $(CuBr)_{1.0037}$ uncoated pellet

The electrical conductivity of CuBr**,** and $CuBr_{1.0037}$ was measured as a function of pressure between 0.5 kbar-32.5 kbar shown in **FIG. 6** shows that conductivity increases with increasing pressure up to 5.0 kbar. The conductivity values of CuBr, and at 5.0 kbar are $27.62 \times 10^{-2}\Omega^{-1}cm^{-1}$, $26.12\times10^{-2}\ \Omega^{-1}cm^{-1}$ and $25.74\times10^{-2}\Omega^{-1}cm^{-1}$, respectively. Beyond this pressure there is an abrupt increase in conductivity evident in **FIG. 6**. The pressure range for this transition appears to be 7.5 kbar to 12.5 kbar. The conductivity values of CuBr, and $CuBr_{1.0037}$ at 12.5 kbar ($95.1\times10^{-2}\ \Omega^{-1}cm^{-1}$, $87.11\times10^{-2}\ \Omega^{-1}cm^{-1}$ and $85.7\times10^{-2}\ \Omega^{-1}cm^{-1}$, respectively) seems to stabilize and remains constant up to 22.5 kbar, however, another sharper transition occurs when the pressure exceeds 22.6 kbar and the conductivity value of CuBr,and $CCCC_{CCCCCC}$ samples at 22.6 kbar to 32.5 kbar remains constant and are $262 \times10^{-2}\Omega^{-1}cm^{-1}$, $254.7\times10^{-2}\Omega^{-1}cm^{-1}$ and $246.2\times10^{-2}\Omega^{-1}cm^{-1}$, respectively.

These two transitions are clearly observed in the conductivity vs pressure plot as shown in **FIG. 6**. From the figure, it is also observed that the value of conductivity in the first transition is not as sharp as in the second transition.

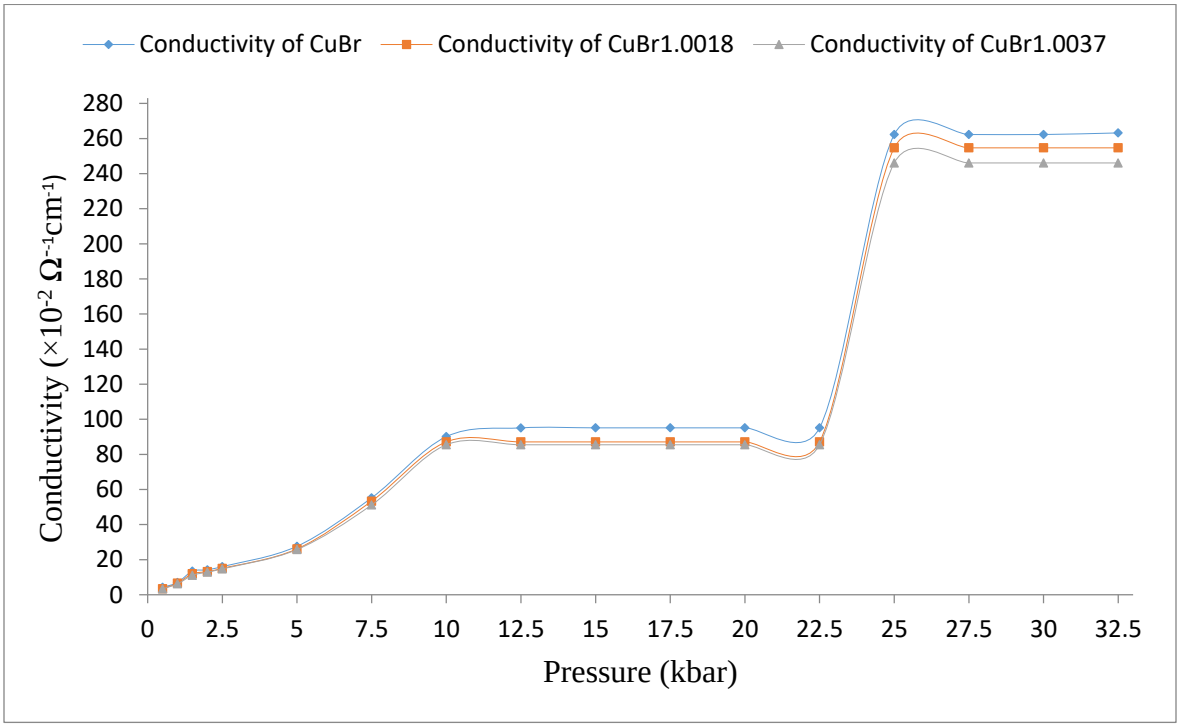

FIG. 6. Plots showing variation of conductivity with pressure (kb).

Conductivity of CuBr, $CuBr_{1.0018}$ and $CuBr_{1.0037}$ pellet coated with graphite

The conductivity of 4 mm graphite coated pellet and (4 mm) stacked pellet (2 mm) are shown in **FIG. 7**. In spite of strong similarity between coated and uncoated samples **(FIG. 6 and FIG. 7)** there are some striking differences between the two, such as (i) onset pressure of both transition in graphite coated sample shift from 7.5 kbar-12.5 kbar to 0.4 kb – 0.8 kb and from 2.5 kbar to 22.0 kbar with much sharper transition, and (ii) values of conductivity in coated samples are a higher order of magnitude in lower pressure range though it almost equalizes in the second transition. The conductivity of single graphite coated pellets of CuBr, $CuBr_{1.0018}$ and $CuBr_{1.0037}$ are raises abruptly (more than twice) from 62.7×10^{-2}, 60.2×10^{-2} $\Omega^{-1}cm^{-1}$, 57.88×10^{-2} $\Omega^{-1}cm^{-1}$ at 0.2 kbar to 136.81×10^{-2} $\Omega^{-1}cm^{-1}$, 130.86×10^{-2} $\Omega^{-1}cm^{-1}$, 125.42×10^{-2} $\Omega^{-1}cm^{-1}$ at 2.0 kbar giving first transition. This value remains constant till pressures exceed 2.0 kbar to set in the second transition at pressure 2.8 kbar attained the highest values of conductivity of CuBr, $CuBr_{1.0018,}$ and $CuBr_{1.0037}$ as 344×10^{-2} $\Omega^{-1}cm^{-1}$, 250.83×10^{-2} $\Omega^{-1}cm^{-1}$ and 231.54×10^{-2} $\Omega^{-1}cm^{-1}$, respectively. These curves also show that the specific conductivity of a single pellet is greater than stacked pellet having the same thickness in the entire pressure range. Stacked pellets after reducing the pressure were separated easily. The conductivity data of CuBr, $CuBr_{1.0018,}$ and $CuBr_{1.0037}$ with graphite coat of single and stacked pellets of equal thickness are shown in **FIG. 7**. The phase transition of graphite coated pellets from observed at very low pressure compared to graphite uncoated pellet **(FIG.6)**. The observed values of conductivity in coated samples are higher in lower pressure range though it almost equalizes in second transition. In **FIG.7** it is also observed that the conductivity of 4 mm pellet of each sample of CuBr is higher than the conductivity of corresponding stacked pellet (2 mm + 2 mm). However, the conductivity decreases with increases of non-stoichiometry of CuBr in both single and stacked pellets.

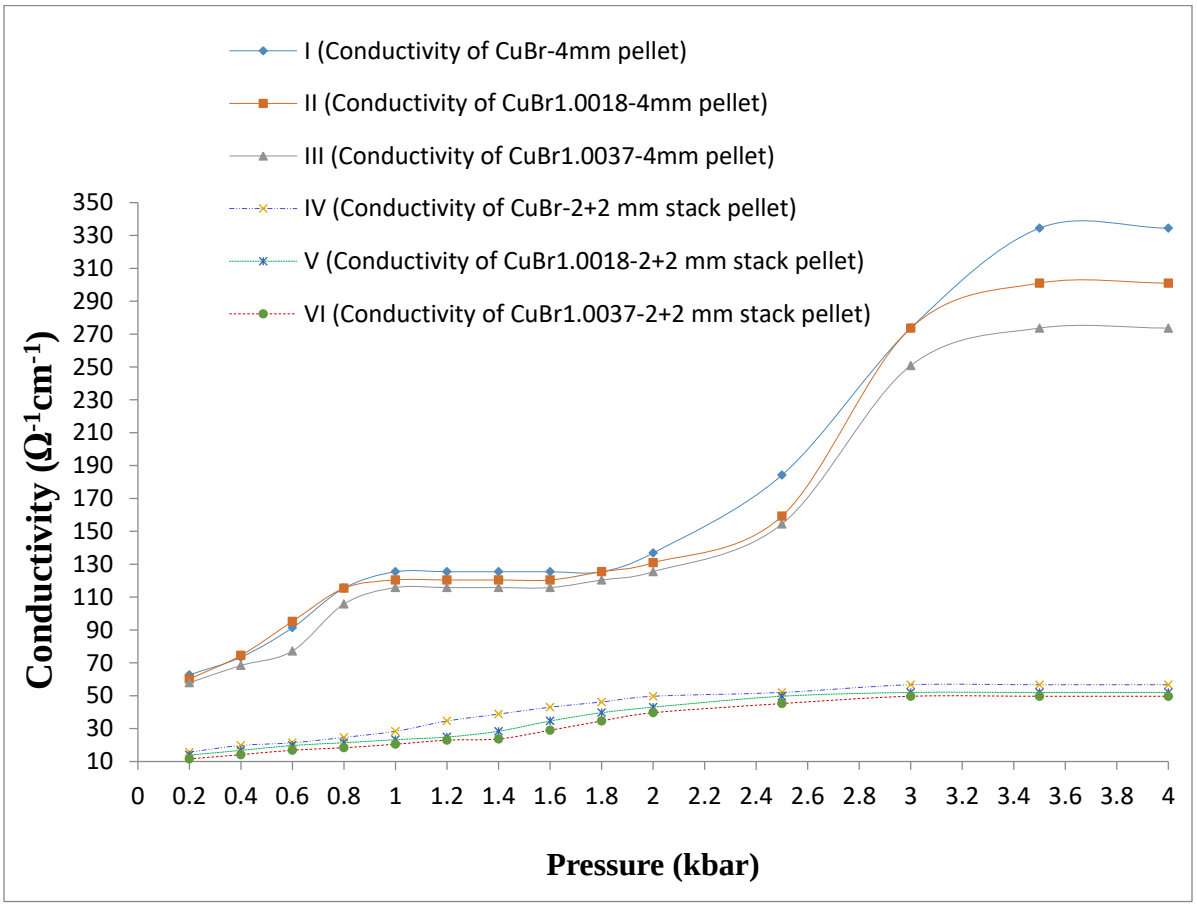

FIG. 7. **Data showing conductivity w.r.t. pressure (pellet coated with graphite paint)**

Conductivity measurement as a function of thickness

The conductivity of CuBr, $CuBr_{1.0018}$ and $CuBr_{1\cdot0037}$ measured as function of thickness of pellet increases at pressure 2.0 kbar, the conductivity of 2 mm, 4 mm and 6 mm pellets are 95×10^{-2} $\Omega^{-1}cm^{-1}$, 93×10^{-2} $\Omega^{-1}cm^{-1}$ and 92.1×10^{-2} $\Omega^{-1}cm^{-1}$, respectively whereas for 4 mm pellets observed conductivity data are 114×10^{-2} $\Omega^{-1}cm^{-1}$, 110.6×10^{-2} $\Omega^{-1}cm^{-1}$ and 109.4×10^{-2} $\Omega^{-1}cm^{-1}$, respectively and for 6 mm pellets the observed conductivity data are 139×10^{-2} $\Omega^{-1}cm^{-1}$, 135.7×10^{-2} $\Omega^{-1}cm^{-1}$ and 132.6×10^{-2} $\Omega^{-1}cm^{-1}$, respectively. The other sets at pressure 4.0 kbar, 6.0 kbar and 10.0 kbar also given in **FIG. 8**. Conductivity of CuBr, $CuBr_{1.0018}$ and $CuBr_{1\cdot0037}$ are increases with increasing thickness as well as pressure.

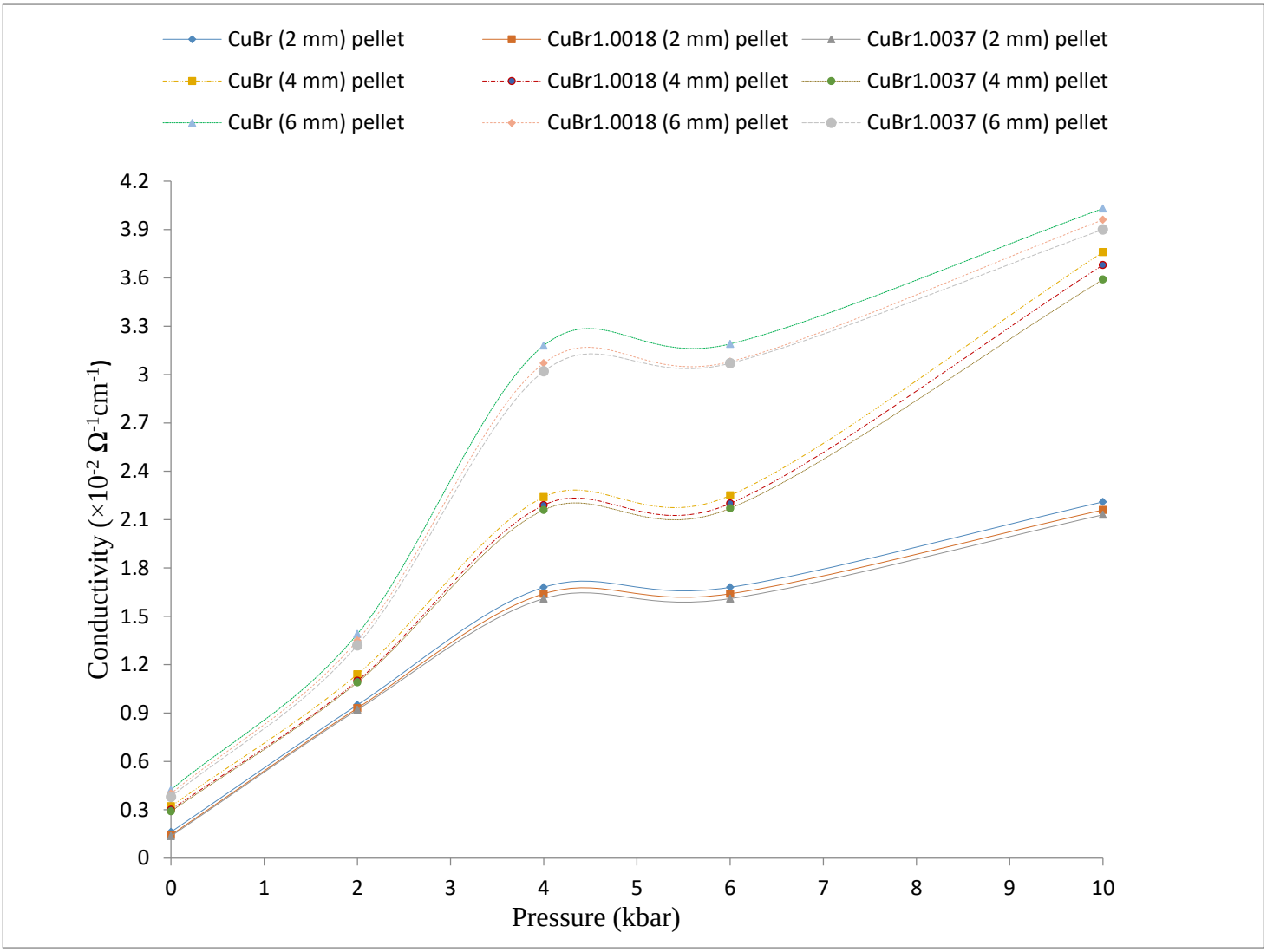

FIG. 8. **Plots showing the effect of thickness on the conductivity against pressure.**

Under this heading plots (CuBr, $CuBr_{1.0018}$ and $CuBr_{1.0037}$) of **FIG. 8** are discussed. The **FIG. 6** is obtained with cell configuration $Cu/CuBr_x/Cu$. Normally linear increased in specific conductivity with reasonable pressure is expected due to enhanced concentration of positive hole or due to narrowing of impurity energy level. But for an abrupt rise in specific conductivity at 7.5 kbar and at 25.0 kbar due to increased hole concentration does not seem to be satisfactory explanation. However, narrowing of impurity energy level cannot be ruled out. It is believed, however, that both transitions one below 10.0 kbar and another above 22.5 kbar are attributed to phase changes of stoichiometric CuBr. Hence, one can expect that as soon as pressure exceeds 7.5 kbar, γ phase (zinc blend structure) changes to β phase (wurzite structure). The such transition appears to be complete at a pressure between 10.0 kbar<P<12.5 kbar. On further increasing the pressure, the material in β phase changes to α phase at 25.0 kbar. The phase diagrams of CuBr to 32.5 kbar consist of three solid phases. The stability region of hexagonal CuBr is terminated at 22.5 kbar. At higher pressures, there is a direct transition from the zinc-blende structure to disordered bcc (α-phase**).** In curve $CuBr_{1.0018}$ and curve $CuBr_{1.0037}$ lower values of conductivity compared to CuBr, in β phase seem to be understandable if we consider that hole concentration in $CuBr_{1.0037}$ would be greater than $CuBr_{1.0018}$.

The conductivity data of CuBr, $CuBr_{1.0018,}$ and $CuBr_{1.0037}$ with graphite coated of single and stacked pellets of equal thickness are shown in **FIG. 7**. The phase transition of graphite-coated pellets from $\gamma \rightarrow \beta$ and $\beta \rightarrow \alpha$ observed at very low pressure compared with graphite uncoated pellet. The observed values of conductivity in coated samples are higher in the lower pressure range though

it almost equalizes in the second transition. In **FIG. 7**, it is also observed that the conductivity of 4 mm pellet of each sample of CuBr is higher than the conductivity of the corresponding stacked pellet (2 mm + 2 mm). However, the conductivity decreases with increases non-stoichiometry of CuBr in both single and stacked pellets. The conductivity of CuBr, $CuBr_{1.0018}$ and $CuBr_{1.0037}$ were found that raises abruptly from 62.7×10^{-2} $\Omega^{-1}cm^{-1}$, 60.2×10^{-2} $\Omega^{-1}cm^{-1}$, 57.88×10^{-2} $\Omega^{-1}cm^{-1}$ at 0.2 kbar to 136.81×10^{-2} $\Omega^{-1}cm^{-1}$, 130.86×10^{-2} $\Omega^{-1}cm^{-1}$,125.42×10^{-2} $\Omega^{-1}cm^{-1}$, respectively at 2.0 kbar giving first transition. This value remains constant till pressures exceed 2.0 kbar to set in the second transition giving at pressure 2.8 kbar attained the highest values of conductivity as 344×10^{-2} $\Omega^{-1}cm^{-1}$, 250.83×10^{-2} $\Omega^{-1}cm^{-1}$ and 231.54×10^{-2} $\Omega^{-1}cm^{-1}$ for CuBr, $CuBr_{1.0018}$ and $CuBr_{1.0037}$, respectively.

Conductivity of CuBr as a function thickness

Results of conductivity as a function of thickness of CuBr pellets described in the previous section can be explained as follows:

The increase of conductivity (σ) with thickness is surprising. Such data are shown in FIG. 7 and FIG. 8. The fact is that conductivity increases with the thickness of the pellet, whether pellets are stacked together to increase the thickness or a single pellet of the same thickness is employed, though for single pellet conductivity is always higher than the stacked pellet. Since measurements were made at room temperature and pressure below 10.0 kbar the sample is expected to be in phase. Enhancement of conductivity with a thickness of pellet either single or stacked is beyond experimental error and represents unusual transport properties of non-stoichiometric CuBr which has not been reported in the literature. Enhancement of conductivity may be due to surface or bulk resistance of the pellet. With available information, we suggest that lower sp. conductivity of stacked pellet of the same thickness is due to larger contact resistance in the stacked pellet. For higher sp. conductivity observed in our sample is attributed to higher mobility of positive holes in the hexagonal layer structure.

Conclusion

Conductivity of CuBr, $CuBr_{1.0018,}$ and $CuBr_{1.0037}$ are increases with increasing thickness as well as pressure. The increase of conductivity (σ) with thickness is surprising. With available information, we suggest that the lower conductivity of stacked pellets of the same thickness is due to larger contact resistance in stacked pellet. For higher conductivity observed in our sample is attributed to higher mobility of positive holes in hexagonal layer structure. The order of magnitude of conductivity is the same, however, the electrical conductivity follows the sequences CuBr>$CuBr_{1.0018}$>$CuBr_{1.0037}$ which is attributed decreases electrical conductivity.

REFERENCES

1. Tubandt C. Handbuch der Experimentalphysik. Akad,Verlagsgesellschaft, Leipzig. 1932;12(1).
2. Vine BH, Maurer RJ. The electrical properties of cuprous iodide. Zeitschrift für Physikalische Chemie. 1951;198(1):147-156
3. Wagner JB, Wagner C. Electrical conductivity measurements on cuprous halides. The J. of Chem Phys.1957; 26(6): 1597-1601
4. Wagner C. Solubility Relations in Ternary Solid Solutions of Ionic Compounds, J Chem Phys. 1950;18(1):62-68.
5. Marina LI, Nashel'skii AY. Thermochemical constants of AIIIBV compound semiconductors, and approximate methods of calculation. Russ. Chem. Rev. 1971;40(7):608.
6. Koch E, Wagner C. The mechanism of ionic conduction in solid salts on the basis of the disorder idea. Z. Phys. Chem.(Leipzig) B. 1937;38:295-324.
7. Friederich E, Meyer W. Metallic conductivity in firm halogenides. Z. Fur Elektrochem. Angew. Phys. Chem.. 1926;32:566-576.
8. Rapoport E, Pistorius CW. Phase diagrams of the cuprous halides to high pressures. phys. rev. 1968;172(3):838.
9. Van Valkenburg A. High Pressure Microscopy of the Silver and Cuprous Halides. J. Res. Natl. Bur. Stand., Phys. Chem.. 1964;68(1):97.
10. Edwards AL, Drickamer HG. Effect of pressure on the absorption edges of some III-V, II-VI, and I-VII compounds. Phys. Rev.. 1961;15;122(4):1149.

11. Jayaraman A, Newton RC, Kennedy GC. Melting and polymorphism of indium antimonide at high pressures. Nature. 1961;191(4795):1288-1290.
12. Moore MJ, Kasper JS, Bundy FP. High pressure phases of CuI. J. Solid State Chem. 1970;1;1(2):170-172.
13. Wojakowska A. Phase equilibrium diagram for the tin (II) bromide-copper (I) bromide system. J. therm. anal.1989;35(1):91-97.
14. Safadi R, Riess I, Tuller HL. Electrical measurements on CuBr. Solid State Ion. 1992 1;57(1-2):125-131.
15. Villain S, Desvals MA, Clugnet G, Knauth P. CuBr by impedance spectroscopy. Solid State Ion. 1996 1;83(3-4):191-198.
16. Harrison LG, Prasad M. Reactivity and catalytic activity of copper chlorides. Part 4.—Electrical properties and acceptor levels produced in CuCl by Cl 2 gas. J. Chem. Soc. Faraday Trans. 1: Phys. Chem. Condens. Ph. 1974;70:471-483.
17. Wajakowska A, Krzyzak E. Electrical conductivity of CuBr in the temperature range 500-1050K. Solid Sate Ion. 2005; 176(37-38):2711-2716 (17).
18. Prasad M. Electrical properties and defect structure of cuprous chloride (Doctoral dissertation, University of British Columbia).
19. Suyal G. Synthesis of nanocomposite glass-like films containing semiconductor nanocrystals and noble bimetallic colloids by sol-gel route and their characterisation. Thesis 2002.
20. Suyal G, Mennig M, Schmidt H. Sol–gel synthesis of cuprous halide nanoparticles in a glassy matrix and their characterization. J. Mater. Chem. 2003;13(7):1783-1788.
21. Singh K, Singh VK, Yadav BC. Measurement of the Hall Effect in a CuBr Pellet. Int. J. Chem. Anal. Sci.
22. Singh K., Yadav B.C., Singh V.K. Electrical conductivity of cuprous bromide in the temperature range of 30-490°C, Indian J. of Chem., 2012;51A(8):1090-1094.